Vibrational exciton coupling in homo and hetero dimers of carboxylic acids studied by linear infrared and Raman jet spectroscopy

Katharina A. E. Meyer, and Martin A. Suhm

Citation: J. Chem. Phys. **149**, 104307 (2018); doi: 10.1063/1.5043400
View online: https://doi.org/10.1063/1.5043400
View Table of Contents: http://aip.scitation.org/toc/jcp/149/10
Published by the American Institute of Physics

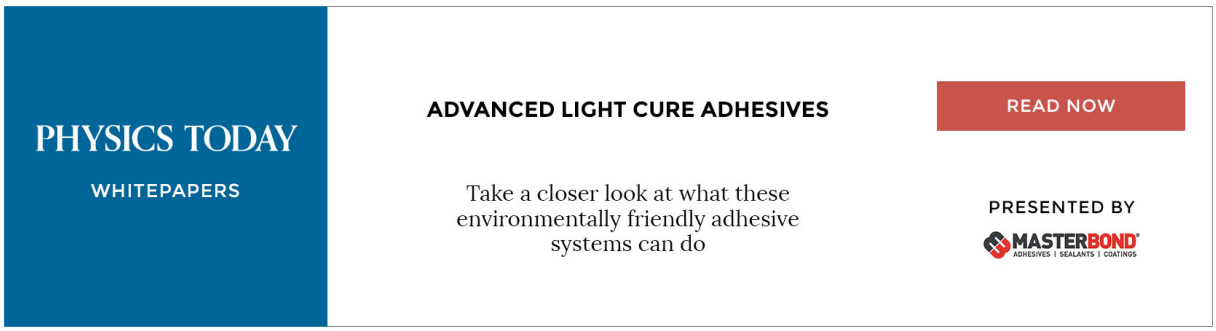

Vibrational exciton coupling in homo and hetero dimers of carboxylic acids studied by linear infrared and Raman jet spectroscopy

Katharina A. E. Meyer and Martin A. Suhm[a)]
Institut für Physikalische Chemie, Universität Göttingen, Tammannstr. 6, 37077 Göttingen, Germany

(Received 8 June 2018; accepted 28 August 2018; published online 13 September 2018)

The jet-cooled band positions of the C=O stretching vibrations in the three hetero dimers composed of formic, acetic, and pivalic acid have been determined. Resonance patterns in the symmetric stretching modes have been corrected for by assuming a single bright state. An analysis of their Davydov or vibrational exciton splitting shows that the hetero dimer values can be averaged from the respective homo dimer splittings (ranging from 56 cm^{-1} for the acetic to 75 cm^{-1} for the formic acid dimer) with an error of ≤7%. The set of 6 exciton splittings and 6 independent downshifts caused by double hydrogen bonding serves as a reference data base for the benchmarking of computational methods. B3LYP is shown to be unable to describe the difference between the formic and acetic acid monomer but is otherwise satisfactory, if one assumes that exciton splittings are only weakly affected by anharmonic effects beyond the deconvoluted local resonances. However, a vibrational perturbation theory test points at significant diagonal anharmonicity effects for the exciton splitting. Spin-component-scaled and canonical MP2 fail in reproducing experimental dimer shifts and splittings in the harmonic approximation, but anharmonic corrections are expected to improve the performance. Harmonic PBEh-3c reproduces the experimental data set well after scaling. The experimental data set the stage for more rigorous anharmonic treatments of the multidimensional coupling of C=O oscillators in carboxylic acid dimers and trimers. In addition, we report the first vibrational jet spectrum of *cis*-formic acid in the C=O stretching region by heating the nozzle and the nozzle feed line of the Raman setup. https://doi.org/10.1063/1.5043400

I. INTRODUCTION

Carboxylic acid dimers form a planar eight-membered ring composed of two linear hydrogen bonds between the OH and the C=O groups and as such represent an exceptionally strong and directional hydrogen bonding motif. The coupling of the equivalent O–H and C=O oscillators in inversion-symmetric dimers results in the so-called Davydov pairs of exclusively IR (a) and Raman (s) active vibrations with splittings Δas. The band pairs are additionally shifted from the corresponding monomer vibrations by Δa and Δs. The splittings arise from the through-space coupling of two initially degenerate monomer vibrations. They provide a sensitive probe for the monomer interaction and intermolecular energy flow and are also denoted vibrational exciton splittings. Both concepts are borrowed from electronic excitons and Davydov splittings in the solid state,[1] and indeed, carboxylic acid dimers may be viewed as elementary models of vibrations in molecular crystals, particularly accessible to theoretical modeling. These dimer vibrations have been extensively characterized by a variety of different experimental techniques.[2–20] Moreover, carboxylic acid dimers, especially the formic acid dimer, have been scrutinized by a vast number of theoretical methods.[21–26] However, the focus of all these characterizations has been on the homo dimers. Keeping in mind that carboxylic acid dimers serve as model systems for double hydrogen bonds in biological systems, where the interacting units usually differ, hetero dimers of carboxylic acids are of interest as well. As opposed to homo dimers, hetero dimers exhibit a permanent electrical dipole moment and thus are particularly suited for a characterization with microwave spectroscopy, especially as the nonpolar homo dimers present in the mixture do not interfere. A manifold of different hetero dimers has been studied, beginning with the hetero dimer consisting of formic and trifluoroacetic acid, by Costain and Srivastava in 1961,[27] followed by further studies.[28–31] Other examples include formic and acetic acid,[32] formic and benzoic acid,[33] formic and propiolic acid,[34] formic and nitric acid,[35] formic and cyclopropanecarboxylic acid,[36] formic and perfluorobutyric acid,[37] acetic and trifluoroacetic acid,[28,30,31] acrylic and trifluoroacetic acid,[38] and difluoroacetic and acrylic acid.[39] As vibrational spectroscopy is sensitive to both homo and hetero dimers, it is more valuable in the exploration of additivity rules than microwave spectroscopy. However, in stark contrast to the homo dimers, very few hetero dimers have been analyzed by vibrational spectroscopy. Keller[40] has examined the mixed dimer composed of formic and trifluoroacetic acid with mid-infrared spectroscopy at room temperature. Apart from that, two further studies

[a)]Electronic mail: msuhm@gwdg.de. Telephone: (+49)551/39-33111. Fax: (+49)551/39-33117.

employing near-infrared spectroscopy[41] and far-infrared spectroscopy[42] exist for hetero dimers. In supersonic jets, only the vibrations in the mixed dimer of formic and benzoic acid have been explored by dispersed fluorescence.[43] More indirectly related and not addressing the exciton coupling issue, 9-hydroxy-9-fluorenecarboxylic acid has been combined with a range of aliphatic acids in the alcoholic OH stretching region by IR/UV spectroscopy.[44] The present work tries to fill this gap by exploring the vibrational characterization of the three hetero dimers composed of formic, acetic, and pivalic acid with linear FTIR and Raman jet spectroscopy with a focus on their C=O stretching vibrations. This initial focus is motivated by the expected absence of extensive Fermi resonance distorting the local modes and the presence of substantial Davydov coupling. It should form a suitable reference point for studies at lower[13] and higher frequencies.[45] Aside from analyzing the Davydov splitting and the downshift of the respective C=O stretching vibrations of the dimers with respect to the monomer, the additivity of the mode coupling shall be explored, i.e., the accuracy of the prediction of the hetero dimer values from the arithmetic average of those of the homo dimers. Besides, the obtained set of six Davydov splittings and spectral downshifts also represents a suitable reference for benchmarking purposes, as any systematic monomer error cancels for the Davydov couplings, whereas it is included in the shifts. An open question is whether Davydov couplings are less susceptible to anharmonic corrections than fundamental modes and dimerization shifts. It is conceivable that symmetric (Raman active) distortion involves more diagonal anharmonicity because it senses the double-minimum nature of the hydrogen bond potential. Even if there is such a systematic anharmonic contribution, it can be worked out for the simplest dimer[46] and then probably be transferred to larger homo and hetero dimers. In this way, quantum chemical approximations for the interaction between molecules can be tested at the easily accessible harmonic force field level. The present experimental results can thus trigger an in-depth theoretical characterization of double hydrogen bonding and we offer a few initial examples.

With regard to carboxylic acid monomers, there is a lack of vibrational gas phase data for the higher-energy *cis*-form. Apart from one high-resolution FTIR gas phase study of the torsional ν_9 mode of *cis*-formic acid by Baskakov *et al.*,[47] there is to our knowledge no vibrational gas phase data in other spectral regions. In rare gas matrices, however, seven of the nine fundamental bands of *cis*-formic acid have already been assigned in 1997 by Pettersson *et al.*,[48] followed by numerous further studies.[49–56] Consequently, recent anharmonic theoretical studies by Tew and Mizukami[57] as well as Richter and Carbonnière[58] still had to compare their data to these perturbed band positions. As an attempt to narrow this discrepancy between matrix and gas phase vibrational data, we present the first Raman jet spectrum of *cis*-formic acid in the C=O stretching region obtained by heating the nozzle and the respective nozzle feed line. The determined band position is 10 cm^{-1} higher in wavenumber compared to the matrix data[48] and lies directly in between the results of both theory groups, further highlighting the need for additional jet data.

II. EXPERIMENTAL AND THEORETICAL METHODS

The FTIR and the Raman jet setups used throughout this work are briefly summarized here. More detailed descriptions can be found in Refs. 59 and 60, respectively. Both setups exhibit a similar sample preparation—the condensed carboxylic acids (formic: Emsure, 98%–100%, acetic: Acros Organics, 99.8%, and pivalic acid: Alfa Aesar, 99%) are supplied by two cooled saturators. Helium is conducted through the saturators, and the mixtures of carrier gas and gaseous carboxylic acid are filled into the reservoir from which the supersonic expansion takes place through a slit nozzle into the evacuated jet chamber. The mixing ratio of the two acids in the reservoir can be varied. Usually, it is kept reasonably close to 1:1. Carboxylic acid concentrations are estimated from the vapor pressures at the respective temperature. In the case of formic acid, the vapor pressures are estimated from the sublimation enthalpy[61] and the triple point.[62,63] For acetic and pivalic acid, the vapor pressures are obtained from Refs. 64 and 65, respectively. However, one should keep in mind that the thus determined concentrations are upper limits in the sense that equilibrium between the solid or liquid and the gas phase is not fully reached. The concentration uncertainty for solids is larger as the surface area changes to a greater extent in comparison to the liquid. The different monomer-dimer equilibria in the gas phase add to the uncertainty. As the C=O stretching vibration has a reasonably constant IR intensity and Raman scattering cross section across the three investigated homologs, an independent estimate for the mixing ratio is given by the relative strength of the C=O signals of the homo dimers, where they do not overlap (see Figs. 2 and 3).

In the case of the FTIR jet setup, a 600 × 0.2 mm^2 slit nozzle is employed and the gas pulses are synchronized with the spectrometer scans (Bruker IFS 66v) via a pulse generator. A pump rack of 2500 $m^3\ h^{-1}$ pumping speed ensures low background pressures of $p_{bg} \leq 0.2$ mbar in between pulses, and the 23 m^3 jet chamber inhibits pressure peaks larger than 1–2 mbar during pulses. The expansion is probed through CaF_2 optics by a mildly focused IR beam from a Globar, which is modulated by a KBr beam splitter. Behind the nozzle, the IR beam is focused onto an LN_2-cooled HgCdTe (MCT) detector.[59]

The supersonic expansion probed by the 532 nm Raman laser is continuous from a 4 × 0.15 mm^2 slit nozzle with typical background pressures of $p_{bg} \leq 2$ mbar in the jet chamber, which is pumped with 500 $m^3\ h^{-1}$ pumping speed. Unlike the FTIR jet setup, the nozzle and the nozzle feed line are heatable.[66] Unless otherwise noted, both are kept at room temperature. The beam of the Millenia eV 20–25 W laser crosses the expansion perpendicular to the propagation direction of the flow. Throughout this work, the nozzle distance is kept at 1 mm. The scattered radiation is collimated perpendicular to both the expanding flow and the laser by a photographic lens (Nikkor 50 mm, f/1.2) and is then dispersed in a 1.0 meter monochromator. A LN_2-cooled charge coupled device (CCD) camera (Princeton Instruments Spec-10 400B/LN) consisting of 1340 × 400 pixels serves as a detector. The spectral calibration is achieved with neon and krypton emission lines with a resolution of about 1 cm^{-1}. Cosmic ray removal is accomplished by comparison

of several recorded spectra. The recording times of each spectrum amount to 120–300 s. Interaction of the molecules with the Raman laser is restricted to less than 100 ns such that active overtone pumping and subsequent isomerization[67] should be negligible.

The accompanying density functional theory (DFT) calculations have been performed with the Gaussian 09 program package (revision E.01).[68] The hybrid functional B3LYP has been used in combination with Grimme's pairwise dispersion correction (D3) and Becke-Johnson (BJ) damping.[69] Two basis sets, aug-cc-pVTZ (aVTZ) and def2-TZVP, are employed in order to compare their performance with regard to the systems used throughout this work. A comparison of both basis sets can be found in Sec. III C. The two computational levels are chosen to provide a scalable comparability among systems, leaving room for larger assemblies as well. All harmonic band positions are scaled by 0.986 and 0.983, respectively, to the antisymmetric C=O stretching vibration of the formic acid dimer $(FF)_a$. Anharmonic monomer wavenumbers (and in one case dimer wavenumbers) are calculated with the vibrational perturbation VPT2[70] method as implemented in Gaussian 09. Where a pronounced local resonance is predicted (for the symmetric dimer C=O stretch), results before and after the resonance treatment are given.

To explore the agreement of the experimental exciton splittings and shifts with $(FF)_a$-scaled harmonic frequency calculations, additional methods have been tested, namely, the PBEh-3c functional[71] and spin-component-scaled (SCS)-MP2 using the resolution of identity (RI) approximation as implemented in the ORCA program package (version 4.0.1),[72] as well as MP2, M06-2X, and PM3 as implemented in Gaussian 09. The SCS-MP2, M06-2X, and MP2 calculations have been performed with the aVTZ basis set. The results can be found in Sec. III D. For MP2, additional harmonic and VPT2 aVQZ calculations have been performed for the formic and acetic acid monomers (cf. Table V in Sec. III C). More accurate calculations are possible[46,73,74] and encouraged for the simplest representatives. For these, the present experimental data can serve as benchmark references and the data set of up to 6 monomer combinations helps in avoiding fortuitous error cancellation.

III. RESULTS AND DISCUSSION

A. Dimer stabilities

The global minimum structures of the monomers and (homo and hetero) dimers of formic (F), acetic (A), and pivalic acid (P) are depicted in Fig. 1. The in-plane bond at the α carbon always points to the C=O side, as in the monomers. The most stable binding motif of carboxylic acid dimers is the doubly hydrogen bonded structure[4,12,14] that, as expected, remains the global minimum for the hetero dimers (see Fig. 1). In the hetero dimers containing formic acid, the hydrogen bond lengths differ significantly (4–6 pm), whereby the hydrogen bond, where the formic acid acts as the donor, is shorter. In the (AP) hetero dimer, the length of the hydrogen bonds is more uniform with a difference of only 1 pm. The harmonically estimated zero-point corrected dissociation energies (Table I) suggest that the most stable dimer is the pivalic acid dimer, followed by the hetero dimer composed of acetic and pivalic acid. The least stable dimer is the formic acid dimer. The dissociation energy increases with the size of the substituent implying that a large part of the increase in stability of the dimers is due to dispersion interactions. This is supported by a uniform binding energy of 65 ± 1 kJ mol^{-1} for all six dimers obtained by subtracting the respective D3 dispersion energy gain[69] from the electronic dissociation energy.

A large degree of computational additivity is already revealed by predicting the mixed dimer dissociation energies from arithmetic averages of the computed homo dimer values, also listed in Table I. An important aspect of the present work will be to investigate experimentally whether this additivity carries through to mode couplings. The computed absolute dissociation energies may be in error by as much as 10%, as indicated by the anharmonic experimental value of 59.5 kJ mol^{-1} for (FF)[18] and the indication that most of the anharmonic contributions cancel.[74] This also seems to be the case for (AA), when compared to a semiexperimental value[20] of 67–70 kJ mol^{-1}. Therefore, it is essential to turn to experimental quantities in the investigation of mixing rules for carboxylic acid dimers.

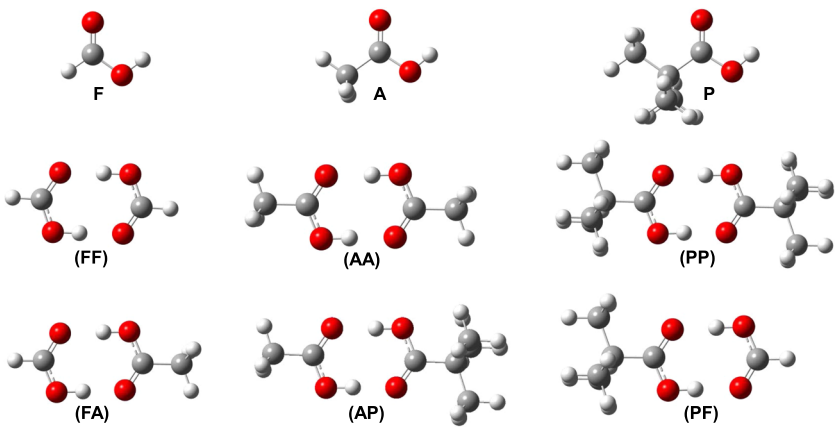

FIG. 1. Global minimum structures of the monomers and (homo and hetero) dimers of formic, acetic, and pivalic acid, calculated at the B3LYP-D3(BJ)/aVTZ level.

TABLE I. Harmonically zero-point corrected dissociation energies D_0^h of the homo and hetero dimers of formic, acetic, and pivalic acid with respect to the most stable monomers, calculated at the B3LYP-D3(BJ)/aVTZ level. In the second column, arithmetic homo dimer averages $\bar{D}_0^h$ are provided for the hetero dimers.

Dimer	D_0^h (kJ mol^{-1})	$\bar{D}_0^h$ (kJ mol^{-1})
(FF)	66.6	
(AA)	71.3	
(PP)	73.3	
(FA)	69.3	69.0
(AP)	72.2	72.3
(PF)	70.4	70.0

B. FTIR and Raman jet spectra

The FTIR jet spectra of the mixtures of formic and acetic [Fig. 2(a.I)], acetic and pivalic [Fig. 2(b.I)], and pivalic and formic acid [Fig. 2(c.I)] are shown in Fig. 2 alongside scaled single substance spectra (red: formic acid, blue: acetic acid, and green: pivalic acid) and the respective difference spectra (orange). The calculated band positions are scaled to the band of the antisymmetric C=O stretching vibration of the formic acid dimer $(FF)_a$ and are each shown below the respective spectra [Figs. 2(a), 2(b), and 2(c.II)]. The calculations have been performed with the larger aVTZ basis set.

The mixture of formic and acetic acid has the smallest calculated band position difference of the respective homo and hetero dimer bands among the three combinations—the hetero dimer band lies directly in between the homo dimer bands with a difference of solely −5 cm^{-1} to $(FF)_a$ and 4 cm^{-1} to $(AA)_a$ [Fig. 2(a.II)]. Slightly larger differences of −6 cm^{-1} to $(AA)_a$ and 8 cm^{-1} to $(PP)_a$ are predicted for the acetic-pivalic acid hetero dimer [Fig. 2(b.II)]. The hetero dimer composed of formic and pivalic acid has the largest predicted band position difference to the respective homo dimers of −13 cm^{-1} to $(FF)_a$ and 10 cm^{-1} to $(PP)_a$ [Fig. 2(c.II)]. In the spectra of all three carboxylic acid combinations, a peak emerges in between the homo dimer peaks that remains when the scaled single substance spectra are subtracted (cf. difference spectra in Fig. 2). The band positions of $(FA)_a$ (1736 cm^{-1}), $(AP)_a$ (1726 cm^{-1}), and $(PF)_a$ (1728 cm^{-1}) are in good agreement with the calculated, $(FF)_a$-scaled band positions with differences lower than 10 cm^{-1}. The largest mismatch among all dimer bands is found for $(PP)_a$ with an underestimation of 6 cm^{-1}. The average mismatch of the calculated, $(FF)_a$-scaled monomer band positions is slightly larger—the formic acid monomer band position is overestimated by 8 cm^{-1} and that of the acetic acid monomer is underestimated by 6 cm^{-1}. By contrast, the pivalic acid monomer band position is accurate to 1 cm^{-1}. Note that a higher level F calculation[74] matches the experiment perfectly, although in the corresponding paper it was compared to an experimental reference value which is off by 67 cm^{-1}. Two reasons for this erroneously large discrepancy are that the reference value was obtained in matrix isolation[50] and that the theoretical authors picked a weak combination band.

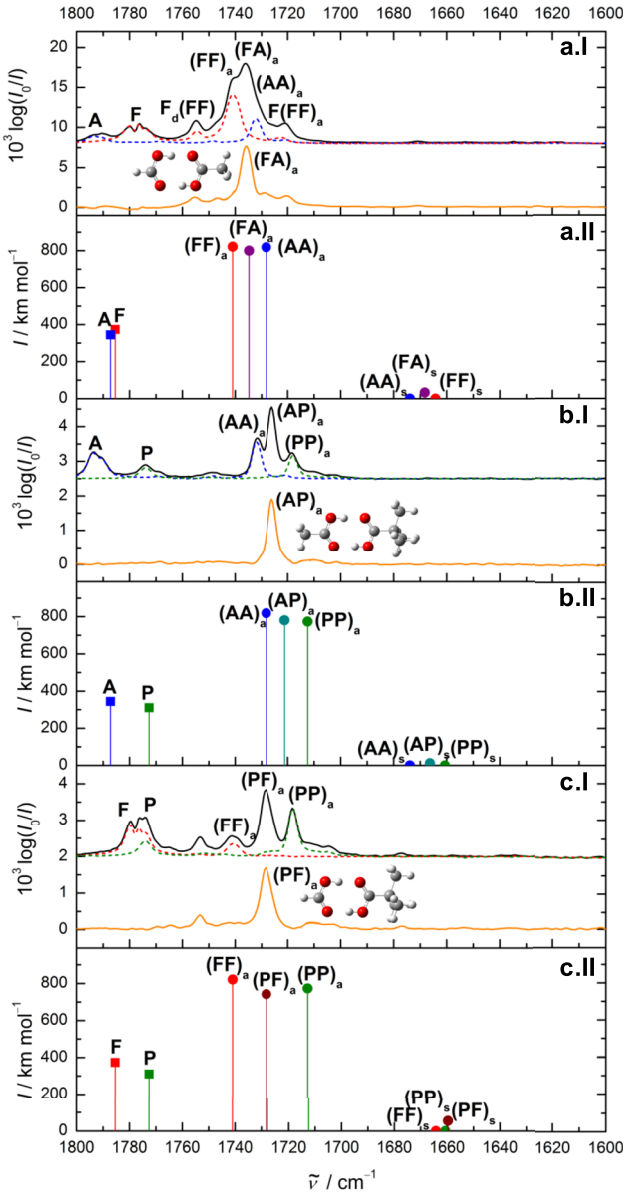

FIG. 2. FTIR C=O stretching jet spectra of formic, F, and acetic acid, A [c_F, c_A < 0.1%, 560 mbar reservoir pressure, (a.I)]; acetic, A, and pivalic acid, P [c_A, c_P < 0.05%, 750 mbar reservoir pressure, (b.I)]; and pivalic, P, and formic acid, F [c_P, $c_F \leq 0.05$%, 560 mbar reservoir pressure, (c.I)] in helium based on 50 pulses. Scaled single substance spectra are depicted with dashed lines (red: F, blue: A, and green: P) and the corresponding difference spectra are shown in orange. The harmonic B3LYP-D3(BJ)/aVTZ band positions (scaled by 0.986) and IR intensities of the respective systems are shown below the spectra [(a), (b), and (c.II)]. F-containing expansions show additional trimer features such as the docking unit vibration F_d(FF); see Ref. 75.

To determine the band positions of the symmetric C=O stretching vibrations of the hetero (and homo) dimers, Raman jet spectra have been recorded for all three combinations (Fig. 3). For both systems containing acetic acid, the B3LYP-D3(BJ)/aVTZ calculations predict that the respective hetero dimer band lies in between the homo dimers [Figs. 3(a.II) and 3(b.II)], with differences of −4 cm^{-1} and 5 cm^{-1} for $(FA)_s$, and of −9 cm^{-1} and 8 cm^{-1} for $(AP)_s$. The symmetric C=O stretching vibration of the hetero dimer composed of formic and pivalic acid is the only hetero dimer band that is downshifted with respect to both homo dimer bands. The predicted downshift to $(FF)_s$ and $(PP)_s$ amounts to 10 cm^{-1} and 2 cm^{-1},

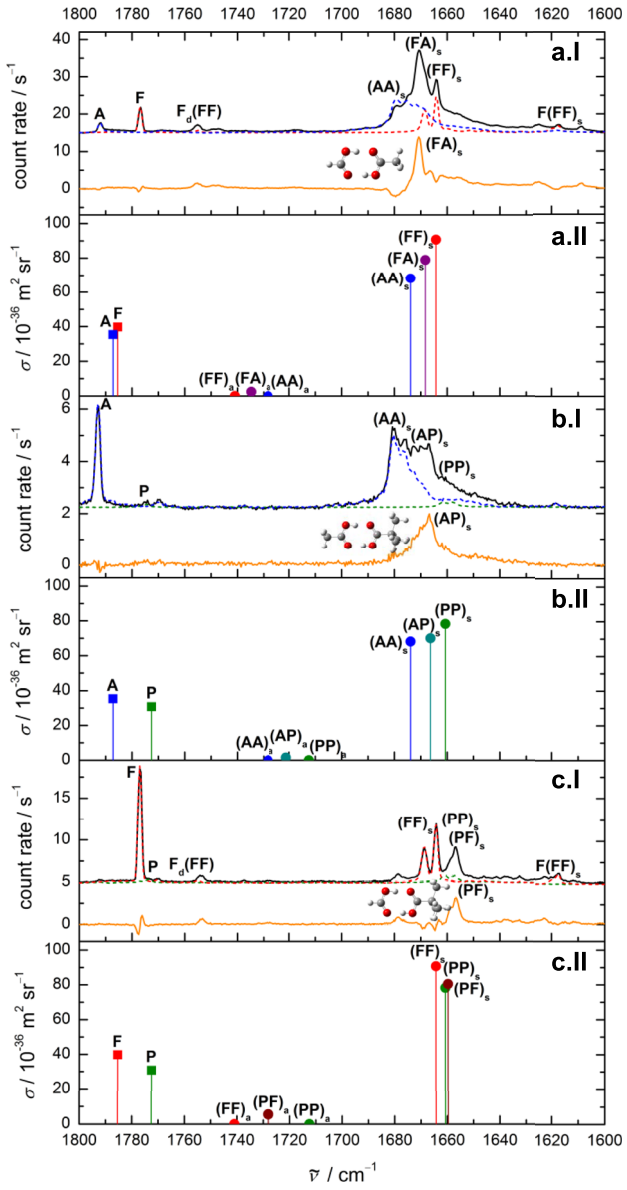

FIG. 3. Raman C=O stretching jet spectra of formic, F, and acetic acid, A [c_F, c_A < 0.4%, 700 mbars reservoir pressure, (a.I)]; acetic, A, and pivalic acid, P [c_A, c_P < 0.05%, 1000 mbars reservoir pressure, (b.I)]; and pivalic, P, and formic acid, F [c_P, c_F < 0.05%, 1500 mbars reservoir pressure, (c.I)] in helium with recording times of 5 × 180 s. Scaled single substance spectra are depicted with dashed lines (red: F, blue: A, green: P) and the corresponding difference spectra are shown in orange. The harmonic B3LYP-D3(BJ)/aVTZ band positions (scaled by 0.986) and IR intensities of the respective systems are shown below the spectra [(a), (b), and (c.II)]. F-containing expansions show additional trimer features such as the docking unit vibration F_d(FF); see Ref. 75.

respectively. Compared to the antisymmetric C=O stretching vibrations, the corresponding symmetric band positions match experiment even better, despite scaling all of them to an antisymmetric band. The largest mismatches are as low as 3 cm^{-1}. The difference spectra formed from the mixed and intensity-scaled single substance spectra exhibit a few irregularities such as negative bands, e.g., for the acetic acid dimer band in Fig. 3(a.I), or residual contributions of homo cluster bands, e.g., for the formic acid dimer band in Fig. 3(a.I). These are caused by slightly varying monomer-to-dimer-ratios in the single substance spectra compared to the mixed spectra. Nonetheless, all three hetero dimer bands can be clearly seen at 1671 cm^{-1} (FA)$_s$, at 1667 cm^{-1} (AP)$_s$, and at 1657 cm^{-1} (PF)$_s$ in both the mixed and the difference spectra. It is expected that imperfect subtraction does not distort the difference band maxima by more than 0.5 cm^{-1}. Consistent with theoretical predictions, the Raman intensity of the IR active bands due to symmetry breaking is negligible. The band positions of the symmetric and antisymmetric C=O stretching vibrations of all homo and hetero dimers are summarized in Table II in comparison to those of Refs. 76–78. As the symmetric C=O stretching vibrations of all homo dimers exhibit features of local anharmonic resonances (cf. Fig. 3), their center of mass has been set as the band position. This corresponds to the assumption that the perturbed states derive all their intensity from the C=O stretch perturbation. In Refs. 76–78, other band center criteria have in part been used. The only deviation larger than 1 cm^{-1}–2 cm^{-1} is found for the symmetric C=O stretching vibration ν_s of the acetic acid dimer with 4 cm^{-1}. In Ref. 76, the intensity maximum of the 1688 cm^{-1}–1662 cm^{-1} band pattern has been assigned as the band position instead of the center of mass. Moreover, as both the band shape and maximum are concentration dependent, lower concentrations of 0.1% compared to the 0.7% of Ref. 76 have been employed to avoid further band distortion by overlapping bands of stacks of dimers. Rewardingly, for formic acid, the presence of mode coupling for the symmetric C=O stretching vibration has also been predicted theoretically.[46]

C. Analysis of fundamental wavenumbers

On an absolute scale, the overall agreement of the $(FF)_a$-scaled harmonic B3LYP-D3(BJ)/aVTZ calculations with the anharmonic experimental monomer and (homo and hetero) dimer bands of the carboxylic acids is satisfactory, as seen in Figs. 2 and 3. Apparently, anharmonicity contributions and electronic structure deficiencies are rather uniform across the modes and systems. Indeed, higher level anharmonic calculations[74] show a similar scatter for F and (FF). However, particularly with regard to larger homo and hetero clusters such as trimers or tetramers, the computational demand needs to be reduced. Since the formic acid trimer bands have been recently assigned,[75] an examination of hetero trimers might help in assigning the acetic and pivalic acid homo trimer bands. Toward this goal, all calculations have also been performed with the smaller def2-TZVP basis set.

TABLE II. Experimental jet-cooled band positions (in cm^{-1}) of the symmetric (s) and antisymmetric (a) C=O stretching vibrations of the (homo and hetero) dimers composed of the formic, acetic, and pivalic acid (deperturbed from anharmonic resonances for ν_s by taking the center of the band multiplet) in comparison to Refs. 76–78.

Dimer	$\tilde{\nu}_a$	$\tilde{\nu}_a$, Reference	$\tilde{\nu}_s$	$\tilde{\nu}_s$, Reference
(FF)	1741	1740.7[77]	1666	1668[76]
(AA)	1732	1732[78]	1676	1680[76]
(PP)	1718	...	1660	1658/1661[76]
(FA)	1736	...	1671	...
(AP)	1726	...	1667	...
(PF)	1728	...	1657	...

TABLE III. Experimental and calculated, dimer-scaled band positions (in cm^{-1}) of the C=O stretching vibration of the formic, acetic, and pivalic acid monomer. The calculations have been performed at the B3LYP-D3(BJ)/aVTZ level (scaling factor 0.986) and at the B3LYP-D3(BJ)/def2-TZVP level (scaling factor 0.983).

		B3LYP-D3	
Monomer	$\tilde{\nu}_{C=O}$	aVTZ	def2-TZVP
F	1777	1785	1787
A	1793	1787	1789
P	1774	1773	1772

TABLE IV. Experimental and calculated, (FF)-ν_a-scaled band positions (in cm^{-1}) of the symmetric $\tilde{\nu}_s$ and antisymmetric $\tilde{\nu}_a$ C=O stretching vibrations of homo and hetero dimers of formic, acetic, and pivalic acid. The calculations have been performed at the B3LYP-D3(BJ)/aVTZ level (scaling factor 0.986) and at the B3LYP-D3(BJ)/def2-TZVP level (scaling factor 0.983).

		B3LYP-D3			B3LYP-D3	
Dimer	$\tilde{\nu}_a$	aVTZ	def2-TZVP	$\tilde{\nu}_s$	aVTZ	def2-TZVP
(FF)	1741	(1741)	(1741)	1666	1664	1665
(AA)	1732	1728	1728	1676	1674	1673
(PP)	1718	1712	1711	1660	1661	1659
(FA)	1736	1735	1735	1671	1668	1668
(AP)	1726	1721	1720	1667	1666	1665
(PF)	1728	1728	1727	1657	1660	1659

A comparison of the two sets of calculated, scaled band positions of the carboxylic acid monomers and dimers (Tables III and IV) shows that both yield similar results. The largest deviation from experiment for both methods can be found for the formic acid monomer band with an overestimation of 8 cm^{-1} and 10 cm^{-1} for aVTZ and def2-TZVP, respectively. The largest underestimation can be found for A and $(PP)_a$—it amounts to 6 cm^{-1} for aVTZ and to 4 cm^{-1} (A) and 7 cm^{-1} [$(PP)_a$] for def2-TZVP. Even though the individual outliers of the calculated band positions are larger for def2-TZVP, the mean absolute deviation is the same (3 cm^{-1}) for both methods. Given other limitations of the B3LYP-D3 approach, this encourages the use of a def2-TZVP basis set for larger clusters, obviously accepting some error compensation between different deficiencies.

For benchmarking and error localization purposes, it makes sense to separate dimer-centered quantities, such as Davydov splittings Δas, where any systematic monomer error cancels, from quantities which do not profit from error cancellation, such as spectral downshifts with respect to the monomer (Δs and Δa). Any mismatch for a single monomer fundamental affects six out of twelve downshift values. Therefore, the pronounced band position mismatch of the formic and acetic acid monomer shall be scrutinized more carefully before turning to dimer benchmarking.

A way of analyzing this deviation is to extend the data set, e.g., taking the higher-energy *cis*-conformation of formic [cF, +15.9 kJ mol^{-1} (B3LYP-D3(BJ)/aVTZ)] and acetic acid [cA, +20.4 kJ mol^{-1} (B3LYP-D3(BJ)/aVTZ)] into account. The *cis*- and the *trans*-conformation of both acids are shown in Fig. 4, whereby one can be converted into the other by torsion of the H around the C–O bond. The *cis*-rotamers of both carboxylic acids have been observed in rare gas matrices by vibrational excitation of the *trans*-form,[48–56] and in the case of formic acid, very weak bands of *cis*-formic acid have also been identified in the gas phase by microwave spectroscopy.[79–81] An experimental energy penalty consistent with the present B3LYP prediction has been obtained. Moreover, the ν_9 band of *cis*-formic acid has been recorded by high-resolution FTIR spectroscopy, which represents its first gas phase detection by vibrational spectroscopy.[47] However, due to the large energy penalty, they have not been observed in supersonic expansions yet. A strategy to increase the amount of *cis*-rotamers in the jet expansions is to heat the nozzle (and the nozzle feed line if isomerization is slow) while measuring the spectra close to the nozzle to achieve a high signal-to-noise ratio. Due to the small beam diameter of the Raman laser compared to the IR beam, Raman jet spectroscopy allows for very selective measurements, i.e., spectra averaged over a very small expansion area (two orders of magnitude lower than for FTIR spectroscopy), as well as measurements at short nozzle distances on the order of 1 mm. As such, Raman spectroscopy is the method of choice for supersonic jet detection of the *cis*-isomer.

Raman jet spectra of formic acid with increasing nozzle temperatures θ_D can be found in Fig. 5 alongside calculated, uniformly scaled band positions (B3LYP-D3(BJ)/aVTZ level) of both monomer conformations (F and cF), the most stable cyclic and acyclic dimer [(FF) and FF], as well as the formic acid trimer [F(FF)]. When the nozzle temperature is increased from room temperature to 110 °C, all cluster signals decrease rapidly, as expected. Only the cyclic dimer and a small fraction of trimer remain. Additionally, two new bands appear, one upshifted (1818 cm^{-1}) and one downshifted (1770 cm^{-1}) compared to the monomer signal. Both signals increase with nozzle temperature. At 170 °C, nearly all cluster signal is gone. Even the formation of the most stable formic acid cluster, the cyclic dimer, is almost completely hindered. The band downshifted compared to the monomer position at 1770 cm^{-1} can most likely be attributed to a hot band of low frequency vibrations of *trans*-formic acid, with the highest contribution from the lowest lying in-plane OCO bending vibration ν_7 (following the Herzberg nomenclature[82]), which has been located at

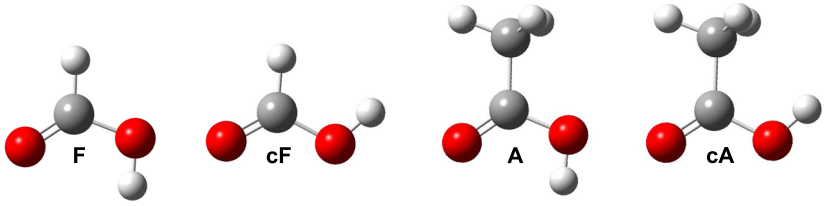

FIG. 4. Minimum structures of the *cis*- and *trans*-rotamers of formic and acetic acid, calculated at the B3LYP-D3(BJ)/aVTZ level.

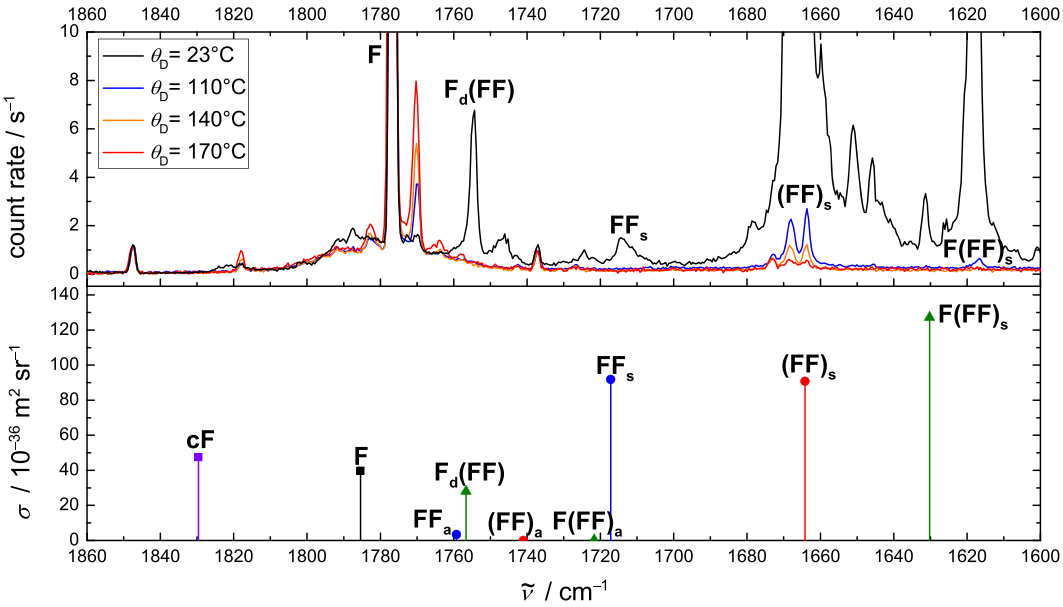

FIG. 5. Upper part: C=O stretching Raman jet spectra of formic acid ($c \approx 0.2\%$) in helium recorded at 1.3 bars stagnation pressure with increasing nozzle temperature (black: 23 °C, blue: 110 °C, orange: 140 °C, and red: 170 °C) with recording times of 300 s. All spectra are scaled to the monomer signal of the spectrum with the lowest nozzle temperature. Lower part: Scaled (0.986) B3LYP-D3(BJ)/aVTZ band positions of the two rotamers (cF and F) of formic acid, the most stable cyclic (FF) and acyclic dimers FF, as well as the formic acid trimer F(FF).

626 cm^{-1} in jet expansions.[76] The calculated anharmonic coupling constant $x_{37} = -6$ cm^{-1} (B3LYP-D3(BJ)/aVTZ VPT2) matches the experimental value of -7 ± 1 cm^{-1}. It disagrees with a previous assignment of the $\nu_3 + \nu_7$ combination band (2376 cm^{-1}) by Freytes and co-workers[83] and Richter and Carbonnière,[58] but a study by Tew and Mizukami[57] attributes this band to $\nu_6 + \nu_7 + \nu_9$. The prediction for $\nu_3 + \nu_7$ (in resonance with $\nu_5 + \nu_6$)[57] is in better agreement with the $\nu_3 + \nu_7 - \nu_7$ hot band found in this work. Clearly, the jet spectra of F deserve a more systematic analysis extending over other spectral ranges, but this is beyond the scope of the present work. The second band at 1818 cm^{-1} differs from the dimer-scaled, calculated band position of the *cis*-rotamer of formic acid by 12 cm^{-1}. This is a slightly larger deviation than that found for the *trans*-conformation (8 cm^{-1}). However, the wavenumber difference between both conformations (41 cm^{-1}) is close to the one found in Ar matrices,[48,50] whereas the matrix shift amounts to about −10 cm^{-1}. Furthermore, assuming similar Raman cross sections, the observed intensity ratio of about 0.01 at 170 °C is consistent with the calculated energy difference between both conformers of +15.9 kJ mol^{-1} (B3LYP-D3(BJ)/aVTZ). As such, the signal at 1818 cm^{-1} can be attributed to the *cis*-rotamer of formic acid and represents its first detection by vibrational jet spectroscopy. It compares quite well to recent anharmonic predictions at 1824 cm^{-1}[57] and at 1810 cm^{-1},[58] respectively. The fact that both studies had to compare their data to the 10 cm^{-1} shifted argon matrix value at 1808 cm^{-1} underlines the significance of this first Raman jet study.

When Raman jet spectra of acetic acid are recorded at nozzle temperatures of 170–190 °C, no additional bands appear that can be attributed to the *cis*-rotamer (Fig. 6). Due to the distinctly larger energy difference between the two rotamers of acetic acid compared to formic acid (20.4 kJ mol^{-1} compared to 15.9 kJ mol^{-1} at the B3LYP-D3(BJ)/aVTZ level), higher nozzle temperatures are required to observe cA, which are currently not accessible with the setup. As a result, solely the *cis*-rotamer of formic acid can be taken into account for a more detailed analysis of the monomer mismatches of formic and acetic acid. It is indicative of a systematic deficiency in the DFT potential energy hypersurface along the C=O stretching coordinate, rather than accidental mode mixing.

Anharmonic frequency calculations using vibrational perturbation theory (VPT2)[70] have been performed for both the *cis*- and the *trans*-rotamer of formic acid as well as for *trans*-acetic acid. These alongside unscaled harmonic values can be found in Table V. Dimer-scaled harmonic band positions are given in parentheses. The methyl torsion in A may serve as an indicator for numerical limitations of the VPT2 approach. In the aVTZ basis, it increases from 72 to 88 cm^{-1} upon anharmonic correction, whereas in the def2-TZVP basis, it decreases from 75 to 34 cm^{-1}. Neither of these trends is very plausible, but we expect that this does not affect the performance for the C=O stretching anharmonicity in a critical way. The anharmonic B3LYP-D3(BJ)/aVTZ as well as B3LYP-D3(BJ)/def2-TZVP C=O stretching frequency calculations for both conformations of the formic acid monomer overestimate the experimental band positions. The difference between the unscaled harmonic and the anharmonic value amounts to 33 cm^{-1} for cF and to 32 cm^{-1} for F for both basis sets. Hence, the anharmonic correction is very similar for aVTZ and def2-TZVP and across the conformations. Moreover, the best agreement between the experimental and calculated band positions is achieved with the anharmonic aVTZ value with differences of solely 5 cm^{-1} and 2 cm^{-1} for cF and F, respectively. In the case of acetic acid, it is the other way around; the anharmonic as well as the scaled harmonic values

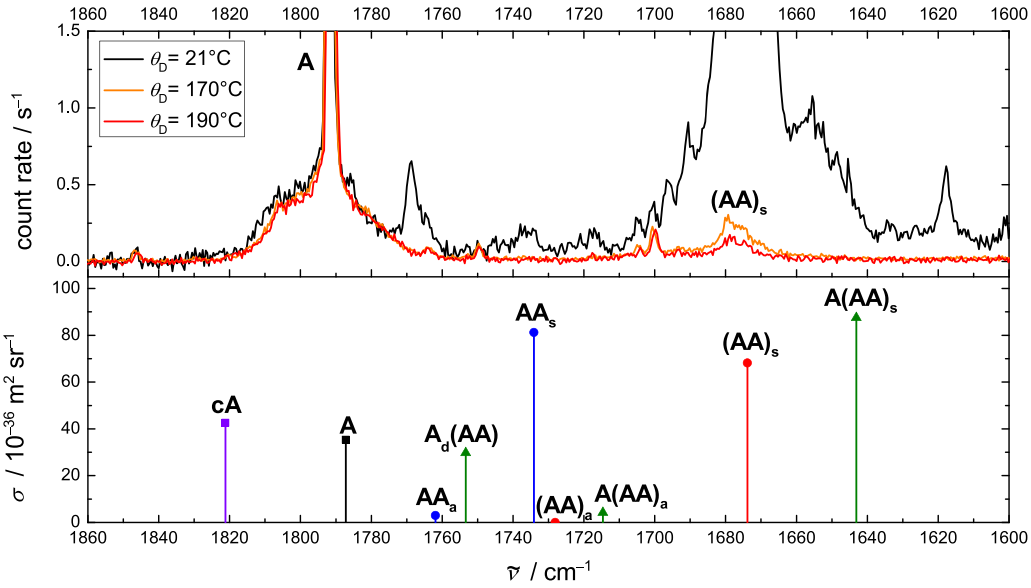

FIG. 6. Upper part: C=O stretching Raman jet spectra of acetic acid ($c \approx 0.1\%$) in helium recorded at 1.0 bar stagnation pressure, recording times of 300 s, and with nozzle temperatures of 21 °C (black), 170 °C (orange), and 190 °C (red). All spectra are scaled to the monomer signal of the spectrum with the lowest nozzle temperature. Lower part: Scaled (0.986) B3LYP-D3(BJ)/aVTZ band positions of the two rotamers (cA and A) of acetic acid, the most stable cyclic (AA) and acyclic dimers AA, as well as the acetic acid trimer A(AA).

generally underestimate the monomer band position. Again, the anharmonic correction is the same (33 cm^{-1}) for both basis sets. Unlike for formic acid, the best overall agreement with the experimental band positions is achieved with the smaller def2-TZVP basis set with differences of 5 cm^{-1} (4 cm^{-1} for the scaled harmonic value). The largest deviation is found for the anharmonic aVTZ value with a mismatch of 13 cm^{-1}. Altogether, each basis set accidentally describes one carboxylic acid slightly better than the other, yet the overall deviations are still moderate. Besides, the prediction of the wavenumber difference between the two rotamers of formic acid is accurate to 4 cm^{-1}. The most striking discrepancy is that all four methods (two basis sets, harmonic and anharmonic) predict the F and A C=O stretching fundamentals within 2 cm^{-1}, whereas experimentally, they are separated by 16 cm^{-1}. It is unlikely that this is due to anharmonic resonances, although the latter are well known in the case of formic acid C=O stretching motion.[84] The uniform VPT2 corrections and small basis set effects suggest that this uniform discrepancy is due to the description of the quadratic part of the potential energy hypersurface by the B3LYP functional. This is confirmed by the MP2/aVQZ results listed in the last columns of Table V. Whereas the absolute performance is inferior to B3LYP, the relative performance for F and A is in much better agreement with experiment. All things considered, the better compromise between accuracy and computational demand is B3LYP-D3(BJ)/def2-TZVP for the carboxylic acids studied in this work once the comparison of C=O stretching fundamentals between F and A is avoided.

D. Excitonic shifts and couplings

After having assigned the symmetric (s) and antisymmetric (a) C=O stretching vibrations of the hetero dimers composed of formic, acetic, and pivalic acid, their Davydov splittings Δas as well as their individual shifts Δa, Δs from monomer positions shall be discussed in comparison to those of the homo dimers. The coupling diagrams of the three combinations are shown in Fig. 7. Since the downshift of the band of the symmetric C=O stretching vibration compared to the

TABLE V. Experimental $\tilde{\nu}_{C=O,\,exp.}$ and calculated harmonic $\omega_{C=O}$ as well as anharmonic $\tilde{\nu}_{C=O}$ (VPT2) band positions (in cm^{-1}) of the C=O stretching vibrations of the two rotamers of formic acid as well as the *trans*-conformer of acetic acid. The calculations have been performed at the B3LYP-D3(BJ)/aVTZ, B3LYP-D3(BJ)/def2-TZVP, and MP2/aVQZ level. Dimer-scaled harmonic band positions are given in parentheses (scaling factor: B3LYP-D3(BJ)/aVTZ: 0.986, B3LYP-D3(BJ)/def2-TZVP: 0.983, MP2/aVQZ: 0.981).

		B3LYP-D3				MP2	
		aVTZ		def2-TZVP		aVQZ	
Monomer	$\tilde{\nu}_{C=O,\,expt.}$	$\omega_{C=O}$	$\tilde{\nu}_{C=O}$	$\omega_{C=O}$	$\tilde{\nu}_{C=O}$	$\omega_{C=O}$	$\tilde{\nu}_{C=O}$
cF	1818	1856(1830)	1823	1865(1833)	1832	1837(1802)	1802
F	1777	1811(1785)	1779	1819(1787)	1787	1798(1764)	1765
A	1793	1813(1787)	1780	1821(1789)	1788	1814(1780)	1784

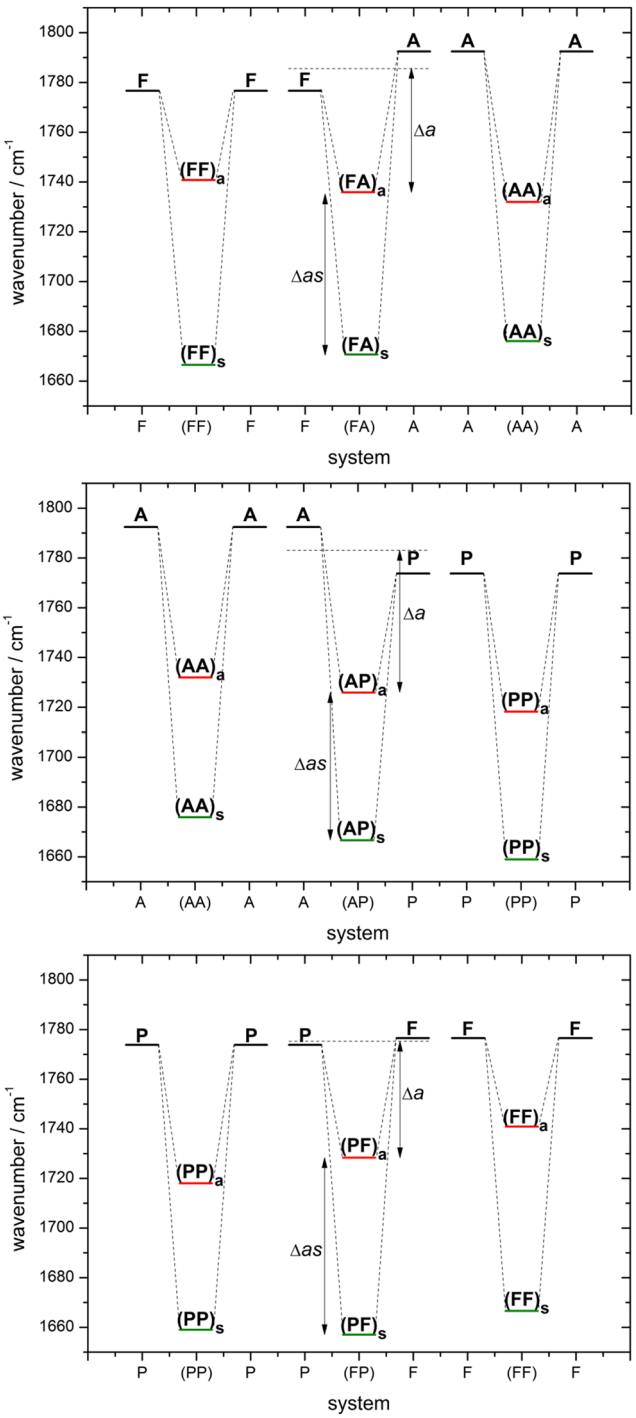

FIG. 7. Exciton coupling of the symmetric and antisymmetric C=O stretching vibrations of the homo and hetero dimers of formic, acetic, and pivalic acid. The harmonic (FF)-ν_a-scaled band position can be found in Tables III and IV.

monomer band position Δs can be calculated from Δa and Δas, it will not be addressed in detail. The experimental and calculated values for Δa and Δas can be found in Table VI. The largest exciton coupling Δas among all dimers can be found for the formic acid dimer with 75 cm^{-1}, directly followed by the hetero dimer composed of formic and pivalic acid with 72 cm^{-1}. The splitting of the third dimer containing formic acid, the hetero dimer composed of formic and acetic acid, is slightly smaller (65 cm^{-1}). The Δas value of the hetero dimer composed of acetic and pivalic acid as well as the respective homo dimer values are with 59 cm^{-1} (AP), 58 cm^{-1} (PP), and 56 cm^{-1} (AA) even lower. The values thus span a wider relative range than binding energies (Table I) or C=O stretching wavenumbers (Table II), which is favorable for benchmarking purposes. The Δa value order is just the opposite—the by far smallest value can be found for the formic acid dimer with only 36 cm^{-1}. The values of both hetero dimers containing formic acid are with 47 cm^{-1} and 49 cm^{-1} noticeably larger (cf. Table VI). The largest downshift compared to the monomer band position can be found for the acetic acid dimer with 61 cm^{-1}. In fact, the acetic acid dimer is the only dimer where the downshift Δa exceeds the exciton coupling Δas. The Δa and Δas values of (PP) and (AP) are similar, whereby Δas is in each case slightly larger (cf. Table VI). For (FA), Δa amounts to 75% of Δas. For (PF), this ratio is even smaller (about 65%) and just below 50% for (FF).

Experimental downshifts Δa are overestimated by at most 6 cm^{-1} for B3LYP-D3(BJ)/def2-TZVP predictions, except for (FF), where the monomer mismatch discussed in Sec. III C is large. The deviations between the calculated Δas_c and experimental exciton couplings Δas are, as a rule, even lower with $\leq$4 cm^{-1} ($\leq$7%). The exception is the pivalic acid dimer, where the discrepancy amounts to 6 cm^{-1} (10%). For the formic acid dimer and the hetero dimer composed of formic and acetic acid, Δas is slightly overestimated (1–2 cm^{-1}); for the other homo and hetero dimers, it is slightly underestimated (1–6 cm^{-1}). Perhaps the most uniformly evolving quantity is the difference between the monomer wavenumber (in the case of hetero dimers, the average monomer wavenumber) and the average dimer wavenumber $\Delta a + 0.5\Delta as$ (see the last two columns in Table VI after rounding-off), again confirming that the cohesion between the two monomers is not so sensitive to substitution. Experimentally, it ranges between 82 and 89 cm^{-1}, with (FF) as a drastic outlier at 74 cm^{-1}. This outlier is much less pronounced in the prediction which may be related to a B3LYP deficiency (vide supra).

An empirical approach for predicting the band positions of hetero dimers is to average the corresponding homo dimer values. The hereby obtained $\overline{\Delta a}$, $\overline{\Delta as}$, $\overline{\Delta a_c}$, and $\overline{\Delta as_c}$ values are accurate to 1–2 cm^{-1}, with the exception of Δas and Δas_c of (PF), which are underestimated by 5 cm^{-1}. This corresponds to a deviation of solely 7% in both cases. The mismatch of Δas and $\overline{\Delta as}$ could be a result of the uncertainty of the $(PF)_s$ band position due to its large band width and resonance pattern in the difference spectrum [cf. Fig. 3(c.I)]. However, the identical mismatch of Δas_c and $\overline{\Delta as_c}$ does not support this conjecture. Despite this exception, predicting the hetero dimer values of Δa and Δas from the experimental or harmonically calculated and $(FF)_a$-scaled homo dimer values is strikingly accurate. This is probably a consequence of the systematic compensation of anharmonicity effects when comparing homo and hetero dimer spectra in terms of excitonic shifts and splittings. It facilitates a test of quantum chemical predictions for these important hydrogen bond couplings up to fairly high levels and down to very severe simplifications because it largely removes the uncertainty of anharmonic corrections and introduces a valuable redundancy in the data set.

TABLE VI. Experimental (Δa), harmonically calculated (Δa_c), and homo dimer interpolated ($\overline{\Delta a}$, $\overline{\Delta a_c}$) downshift of the band of antisymmetric C=O stretching vibration of the cyclic dimers compared to the monomer band position as well as experimental (Δas), harmonically calculated (Δas_c), and homo dimer interpolated ($\overline{\Delta as}$, $\overline{\Delta as_c}$) excitonic splitting between the bands of the symmetric and antisymmetric C=O stretching vibrations. The calculations have been performed at the B3LYP-D3(BJ)/def2-TZVP level (scaling factor 0.983). In the case of (FF), additional anharmonic B3LYP-D3(BJ)/def2-TZVP VPT2 calculations (scaling factor 1.004) are listed in parentheses (for the dominant symmetric C=O stretching signal) and brackets (for the resonance-deperturbed C=O stretch) below the harmonic values. For convenience, the downshift of the center of the Davydov pair is listed in the last two columns.

Dimer	Δa	$\overline{\Delta a}$	Δa_c	$\overline{\Delta a_c}$	Δas	$\overline{\Delta as}$	Δas_c	$\overline{\Delta as_c}$	$\Delta a_c + 0.5\Delta as$	$\Delta a + 0.5\Delta as_c$
(FF)	36		46		75		76		74	84
			(54)				(85) [96]			(97) [102]
(AA)	61		61		56		55		89	89
(PP)	56		62		58		52		85	88
(FA)	49	48	54	54	65	66	67	66	82	88
(AP)	57	58	61	62	59	57	55	54	87	89
(PF)	47	46	52	54	72	67	69	64	83	87

As a further test, the Δa and Δas values have also been harmonically calculated using the increasingly faster SCS-MP2/aVTZ, M06-2X/aVTZ, PBEh-3c, and PM3 methods, as well as MP2/aVTZ. In all cases, the band positions have been scaled to $(FF)_a$. The mean deviations ($\bar{D}$) of each method with respect to the experimental values are listed in Table VII in comparison to those of B3LYP-D3(BJ)/aVTZ and B3LYP-D3(BJ)/def2-TZVP. The mean absolute deviation of $\bar{D}$ amounts to 3 ± 1 cm^{-1} for all methods employed. Especially SCS-MP2/aVTZ, which has yielded satisfactory results for the downshift of the formic acid OH stretching vibration upon nitrogen complexation,[85] fails to predict either quantity correctly—both Δa and Δas are massively underestimated by -19 cm^{-1} and -17 cm^{-1}, respectively. MP2/aVTZ behaves similarly with underestimations of -13 cm^{-1} and -11 cm^{-1}. However, one should note that for both methods only five of the six dimers were taken into account due to the high computational demand of the pivalic acid dimer. Furthermore, it is probable that diagonal anharmonicity of the C=O stretch acts to attenuate the underestimation because the dimer is likely to be somewhat more anharmonic than the monomer and the symmetric stretch is likely to be somewhat more anharmonic than the antisymmetric stretch. Therefore, the apparently better performance of B3LYP compared to MP2 may just be due to error compensation from the neglect of anharmonicity. Nonetheless, this underestimation of experimental Davydov couplings and shifts is only surpassed by harmonically evaluated PM3 with -27 cm^{-1} and -31 cm^{-1}. The other methods tend to overestimate the downshift (if it is not predicted correctly), with two exceptions for PBEh-3c, where Δa for (AA) is underestimated by -4 cm^{-1} and (AP) by -1 cm^{-1}, and one exception for B3LYP-D3(BJ)/aVTZ, where Δa of (AA) is underestimated by -2 cm^{-1}. In the case of the exciton splitting, PBEh-3c is the only method of the four that solely underestimates Δas. For B3LYP-D3(BJ)/def2-TZVP, B3LYP-D3(BJ)/aVTZ, and M06-2X/aVTZ, both overestimation and underestimation of Δas occur, whereby the underestimation predominates for the B3LYP-D3 methods and the overestimation for M06-2X/aVTZ. In total, PBEh-3c performs better than B3LYP-D3(BJ)/def2-TZVP and B3LYP-D3(BJ)/aVTZ in predicting Δa and slightly worse for the exciton splitting Δas. All these comparisons imply that there is no significant anharmonic contribution to Δas besides the resonance multiplet in the symmetric stretch, which was effectively deconvoluted in this work. As discussed above, any diagonal anharmonicity correction is likely to make the entries in Table VII somewhat more positive. This will degrade the performance of the density functionals and improve the performance of the MP2 approaches. This should be carefully investigated in the future, and the observation that similar performance can be achieved for inexpensive and more elaborate methods encourages such an anharmonic study. For the formic acid dimer, additional B3LYP-D3(BJ)/def2-TZVP VPT2 calculations (cf. Table VI) show a distinctly inferior agreement with the experimental Δa and Δas values compared to the harmonic case, in particular if the local resonance for the symmetric C=O stretch is removed (values in brackets instead of parentheses). If VPT2 at this level is to be trusted, this implies that the rather satisfying agreement of the $(FF)_a$-scaled B3LYP-D3(BJ)/def2-TZVP (and B3LYP-D3(BJ)/aVTZ) calculations is a result of error compensation.

TABLE VII. Mean deviation ($\bar{D}$) (in cm^{-1}) of harmonic ν_a(FF)-scaled B3LYP-D3(BJ)/def2-TZVP (scaling factor 0.983), B3LYP-D3(BJ)/aVTZ (0.986), MP2/aVTZ (0.983), SCS-MP2/aVTZ (0.978), M06-2X/aVTZ (0.956), PBEh-3c (0.917), and PM3 (0.904) with respect to the experimental values of Δa and Δas of the six homo and hetero dimers. The mean absolute deviation of $\bar{D}$ across all investigated dimers amounts to 3 ± 1 cm^{-1} for all methods used. In the case of SCS-MP2/aVTZ and MP2/aVTZ, an asterisk (*) denotes that only five of the six dimers are considered, as the pivalic acid dimer is computationally too demanding for the methods.

Method	Δa	Δas
B3LYP-D3(BJ)/def2-TZVP	5	−2
B3LYP-D3(BJ)/aVTZ	3	−2
MP2/aVTZ*	−13	−11
SCS-MP2/aVTZ*	−19	−17
M06-2X/aVTZ	6	3
PBEh-3c	0	−5
PM3	−27	−31

It is of interest to analyze the performance of a recent full-dimensional formic acid dimer potential energy hypersurface[46] in terms of Δas. Harmonically, it predicts a value of 65 cm^{-1} which is close to a somewhat lower level CCSD(T)-F12 *ab initio* prediction in the same work. Anharmonically, using a vibrational configuration interaction (VCI) method, a number of resonances are found in the symmetric C=O stretch, qualitatively in line with experiment (this work and Ref. 75) and with our exploratory VPT2 calculation. As no theoretical Raman intensities are reported, we can only provide a range of 48–92 cm^{-1}. Comparison in that work was made with regular gas phase experiments.[3,10] The present jet data would actually reduce the fundamental wavenumber discrepancy by about 5 cm^{-1}, but the thermal shifts essentially cancel for Δas in this case. Therefore, the predicted harmonic Δas value of 65 cm^{-1} can be compared to the experimental value (75 cm^{-1}) with little influence by thermal excitation in this particular case. The match is perfect if the nominal VPT2 corrections extracted from Table VII are implied and still satisfactory if the VPT2 deperturbation of the local resonance is included. A more detailed analysis of the coupling at higher computational levels is clearly indicated.

IV. CONCLUSIONS

Within this work, the band positions of the C=O stretching vibrations of the three hetero dimers composed of formic, acetic, and pivalic acid have been determined for the first time in supersonic expansions with FTIR and Raman spectroscopy besides the corresponding homo dimers, where only partial analyses existed so far.[20,76–78] For the symmetric stretching fundamentals, it was necessary to deconvolute local resonance patterns under the assumption of a single bright state. It was shown that the formic acid dimer exhibits the largest exciton coupling between the two modes amongst all homo and hetero dimers. The smallest Davydov splitting at three quarters of the formic acid value is found for acetic acid. On the basis of the arithmetically averaged dimerization shifts Δa and splittings Δas of the respective homo dimers, those of the hetero dimers were predicted with an accuracy of ≤7%. In nearly all cases, the accuracy of this combination rule exceeds that of the B3LYP-D3(BJ)/def2-TZVP calculations. Future work has to show whether or not the trend of decreasing B3LYP-D3 performance for excitonic splittings with increasing size of the substituents (Table VI) continues beyond pivalic acid. The carboxylic acid dimer motif may be viewed as a spacer which is compressed by long range dispersion forces between the substituents, and the excitonic coupling is a sensor of this force. If one omits this dispersion contribution, the remaining double hydrogen bond strength is remarkably stable against substitution. This is likely a consequence of the first-order cancellation between any electron-withdrawing or -donating effects for the OH donor and the C=O acceptor in the same molecule. Excitonic couplings are more sensitive to asymmetric substitution because they probe the difference between the two hydrogen bonds, rather than their sum. Superficially, it appears that C=O exciton splittings in carboxylic acid dimers can serve as experimental benchmarks for harmonic quantum-chemical predictions of hydrogen bond mediated mode coupling, circumventing to a large extent the need for anharmonic reference calculations. This is somewhat reminiscent of the water cluster case.[86] However, future work has to show whether diagonal anharmonicity is systematically larger for the symmetric stretching combination than for the antisymmetric stretching mode, as one might infer qualitatively from the double-minimum potential for proton transfer and as suggested by exploratory VPT2 calculations. Intramolecular vibrational energy redistribution shows such a systematic asymmetry, as evidenced by the experimental spectra.

In the mixed and difference spectra, especially apparent when formic acid is involved (Figs. 2 and 3), additional bands can be seen in the vicinity of the hetero dimer bands. In the case of pure formic acid, it was shown that those are formic acid trimer bands.[75] This might indicate that the additional bands are due to hetero trimer bands. A closer scrutiny of the hetero trimer bands might help in assigning those of the homo trimers of acetic and pivalic acid, which have not been assigned yet. Additionally, the higher-energy *cis*-conformer of formic acid has been detected in a supersonic expansion for the first time by coupling Raman spectroscopy with a heatable nozzle. The significance of unperturbed gas phase data of the fundamental vibrations of *cis*-formic acid is readily apparent by the fact that recent anharmonic theoretical studies[57,58] still had to rely on the matrix isolation data recorded in 1997[48] and 2003,[51] respectively.

ACKNOWLEDGMENTS

The present work is dedicated to the memory of L. Khriachtchev, a true master of formic acid isomerism. It was supported by the German Research Foundation (DFG SU 121/7-1, Project Identifier No. 388861488). We thank Sönke Oswald and Arman Nejad for very valuable discussions and Thomas Forsting for the construction of the heatable feed line.

[1] V. M. Agranovich, *Excitations in Organic Solids*, International Series of Monographs on Physics (Oxford University Press, Oxford, New York, 2009), Vol. 142.
[2] R. C. Millikan and K. S. Pitzer, J. Am. Chem. Soc. **80**, 3515 (1958).
[3] J. E. Bertie, J. Chem. Phys. **76**, 886 (1982).
[4] Y. Maréchal, J. Chem. Phys. **87**, 6344 (1987).
[5] M. Halupka and W. Sander, Spectrochim. Acta, Part A **54**, 495 (1998).
[6] M. Gantenberg, M. Halupka, and W. Sander, Chem. - Eur. J. **6**, 1865 (2000).
[7] T. Häber, U. Schmitt, C. Emmeluth, and M. A. Suhm, Faraday Discuss. **118**, 331 (2001).
[8] F. Ito and T. Nakanaga, Chem. Phys. **277**, 163 (2002).
[9] C. Emmeluth, M. A. Suhm, and D. Luckhaus, J. Chem. Phys. **118**, 2242 (2003).
[10] R. Georges, M. Freytes, D. Hurtmans, I. Kleiner, J. Vander Auwera, and M. Herman, Chem. Phys. **305**, 187 (2004).
[11] W. Sander and M. Gantenberg, Spectrochim. Acta, Part A **62**, 902 (2005).
[12] P. Zielke and M. A. Suhm, Phys. Chem. Chem. Phys. **9**, 4528 (2007).
[13] Z. Xue and M. A. Suhm, J. Chem. Phys. **131**, 054301 (2009).
[14] A. Olbert-Majkut, J. Ahokas, J. Lundell, and M. Pettersson, Chem. Phys. Lett. **468**, 176 (2009).
[15] Z. Xue and M. A. Suhm, Mol. Phys. **108**, 2279 (2010).
[16] K. Marushkevich, L. Khriachtchev, J. Lundell, A. Domanskaya, and M. Rasanen, J. Phys. Chem. A **114**, 3495 (2010).
[17] A. Olbert-Majkut, J. Ahokas, J. Lundell, and M. Pettersson, J. Raman Spectrosc. **42**, 1670 (2011).
[18] F. Kollipost, R. Wugt Larsen, A. V. Domanskaya, M. Nörenberg, and M. A. Suhm, J. Chem. Phys. **136**, 151101 (2012).
[19] F. Ito, J. Mol. Struct. **1091**, 203 (2015).

[20]M. Goubet, P. Soulard, O. Pirali, P. Asselin, F. Réal, S. Gruet, T. R. Huet, P. Roy, and R. Georges, Phys. Chem. Chem. Phys. **17**, 7477 (2015).
[21]S. Miura, M. E. Tuckerman, and M. L. Klein, J. Chem. Phys. **109**, 5290 (1998).
[22]G. M. Florio, T. S. Zwier, E. M. Myshakin, K. D. Jordan, and E. L. Sibert, J. Chem. Phys. **118**, 1735 (2003).
[23]J. Chocholoušová, J. Vacek, and P. Hobza, Phys. Chem. Chem. Phys. **4**, 2119 (2002).
[24]H. Ushiyama and K. Takatsuka, J. Chem. Phys. **115**, 5903 (2001).
[25]N. Shida, P. F. Barbara, and J. Almlöf, J. Chem. Phys. **94**, 3633 (1991).
[26]D. Luckhaus, J. Phys. Chem. A **110**, 3151 (2006).
[27]C. C. Costain and G. P. Srivastava, J. Chem. Phys. **35**, 1903 (1961).
[28]C. C. Costain and G. P. Srivastava, J. Chem. Phys. **41**, 1620 (1964).
[29]G. P. Srivastava and M. L. Golay, J. Phys. B: At. Mol. Phys. **4**, 886 (1971).
[30]E. M. Bellott and E. Wilson, Tetrahedron **31**, 2896 (1975).
[31]L. Martinache, W. Kresa, M. Wegener, U. Vonmont, and A. Bauder, Chem. Phys. **148**, 129 (1990).
[32]M. C. D. Tayler, B. Ouyang, and B. J. Howard, J. Chem. Phys. **134**, 054316 (2011).
[33]L. Evangelisti, P. Ecija, E. J. Cocinero, F. Castano, A. Lesarri, W. Caminati, and R. Meyer, J. Phys. Chem. Lett. **3**, 3770 (2012).
[34]A. M. Daly, K. O. Douglass, L. C. Sarkozy, J. L. Neill, M. T. Muckle, D. P. Zaleski, B. H. Pate, and S. G. Kukolich, J. Chem. Phys. **135**, 154304 (2011).
[35]R. B. Mackenzie, C. T. Dewberry, and K. R. Leopold, J. Phys. Chem. A **118**, 7975 (2014).
[36]A. M. Pejlovas, W. Lin, and S. G. Kukolich, J. Chem. Phys. **143**, 124311 (2015).
[37]J. Thomas, M. J. Carrillo, A. Serrato, W. Lin, W. Jäger, and Y. Xu, J. Mol. Spectrosc. **335**, 88 (2017).
[38]Q. Gou, G. Feng, L. Evangelisti, and W. Caminati, J. Phys. Chem. A **117**, 13500 (2013).
[39]G. Feng, Q. Gou, L. Evangelisti, and W. Caminati, Angew. Chem., Int. Ed. Engl. **53**, 530 (2014).
[40]J. W. Keller, J. Phys. Chem. A **108**, 4610 (2004).
[41]H. E. Affsprung, S. D. Christian, and A. M. Melnick, Spectrochim. Acta **20**, 285 (1964).
[42]D. Clague and A. Novak, J. Mol. Struct. **5**, 149 (1970).
[43]C. K. Nandi, M. K. Hazra, and T. Chakraborty, J. Chem. Phys. **123**, 124310 (2005).
[44]Q. Gu, P. Su, Y. Xia, Z. Yang, C. O. Trindle, and J. L. Knee, Phys. Chem. Chem. Phys. **19**, 24399 (2017).
[45]G. L. Barnes and E. L. Sibert, Chem. Phys. Lett. **460**, 42 (2008).
[46]C. Qu and J. M. Bowman, Phys. Chem. Chem. Phys. **18**, 24835 (2016).
[47]O. I. Baskakov, V.-M. Horneman, J. Lohilahti, and S. Alanko, J. Mol. Struct. **795**, 49 (2006).
[48]M. Pettersson, J. Lundell, L. Khriachtchev, and M. Räsänen, J. Am. Chem. Soc. **119**, 11715 (1997).
[49]M. Pettersson, E. M. S. Maçôas, L. Khriachtchev, J. Lundell, R. Fausto, and M. Räsänen, J. Chem. Phys. **117**, 9095 (2002).
[50]E. M. S. Maçôas, L. Khriachtchev, M. Pettersson, R. Fausto, and M. Räsänen, J. Am. Chem. Soc. **125**, 16188 (2003).
[51]E. M. Maçôas, J. Lundell, M. Pettersson, L. Khriachtchev, R. Fausto, and M. Räsänen, J. Mol. Spectrosc. **219**, 70 (2003).
[52]E. M. S. Maçôas, L. Khriachtchev, M. Pettersson, R. Fausto, and M. Räsänen, J. Chem. Phys. **121**, 1331 (2004).
[53]E. M. S. Maçôas, L. Khriachtchev, M. Pettersson, R. Fausto, and M. Räsänen, Phys. Chem. Chem. Phys. **7**, 743 (2005).
[54]K. Marushkevich, L. Khriachtchev, J. Lundell, and M. Räsänen, J. Am. Chem. Soc. **128**, 12060 (2006).
[55]K. Marushkevich, L. Khriachtchev, and M. Räsänen, J. Chem. Phys. **126**, 241102 (2007).
[56]L. Khriachtchev, J. Mol. Struct. **880**, 14 (2008).
[57]D. P. Tew and W. Mizukami, J. Phys. Chem. A **120**, 9815 (2016).
[58]F. Richter and P. Carbonnière, J. Chem. Phys. **148**, 064303 (2018).
[59]M. A. Suhm and F. Kollipost, Phys. Chem. Chem. Phys. **15**, 10702 (2013).
[60]S. Bocklitz and M. A. Suhm, Z. Phys. Chem. **229**, 1625 (2015).
[61]D. R. Stull, Ind. Eng. Chem. **39**, 517 (1947).
[62]J. W. Stout and L. H. Fisher, J. Chem. Phys. **9**, 163 (1941).
[63]M. D. Taylor and J. Bruton, J. Am. Chem. Soc. **74**, 4151 (1952).
[64]D. Ambrose, J. H. Ellender, C. Sprake, and R. Townsend, J. Chem. Thermodyn. **9**, 735 (1977).
[65]S. P. Verevkin, J. Chem. Eng. Data **45**, 953 (2000).
[66]T. Forsting, H. C. Gottschalk, B. Hartwig, M. Mons, and M. A. Suhm, Phys. Chem. Chem. Phys. **19**, 10727 (2017).
[67]A. Olbert-Majkut, J. Ahokas, J. Lundell, and M. Pettersson, J. Chem. Phys. **129**, 041101 (2008).
[68]M. J. Frisch, G. W. Trucks, H. B. Schlegel, G. E. Scuseria, M. A. Robb, J. R. Cheeseman, G. Scalmani, V. Barone, B. Mennucci, G. A. Petersson, H. Nakatsuji, M. Caricato, X. Li, H. P. Hratchian, A. F. Izmaylov, J. Bloino, G. Zheng, J. L. Sonnenberg, M. Hada, M. Ehara, K. Toyota, R. Fukuda, J. Hasegawa, M. Ishida, T. Nakajima, Y. Honda, O. Kitao, H. Nakai, T. Vreven, J. A. Montgomery, Jr., J. E. Peralta, F. Ogliaro, M. Bearpark, J. J. Heyd, E. Brothers, K. N. Kudin, V. N. Staroverov, R. Kobayashi, J. Normand, K. Raghavachari, A. Rendell, J. C. Burant, S. S. Iyengar, J. Tomasi, M. Cossi, N. Rega, J. M. Millam, M. Klene, J. E. Knox, J. B. Cross, V. Bakken, C. Adamo, J. Jaramillo, R. Gomperts, R. E. Stratmann, O. Yazyev, A. J. Austin, R. Cammi, C. Pomelli, J. W. Ochterski, R. L. Martin, K. Morokuma, V. G. Zakrzewski, G. A. Voth, P. Salvador, J. J. Dannenberg, S. Dapprich, A. D. Daniels, Ö. Farkas, J. B. Foresman, J. V. Ortiz, J. Cioslowski, and D. J. Fox, GAUSSIAN 09, Revision E.01, Gaussian, Inc., 2009.
[69]S. Grimme, S. Ehrlich, and L. Goerigk, J. Comput. Chem. **32**, 1456 (2011).
[70]J. Bloino and V. Barone, J. Chem. Phys. **136**, 124108 (2012).
[71]S. Grimme, J. G. Brandenburg, C. Bannwarth, and A. Hansen, J. Chem. Phys. **143**, 054107 (2015).
[72]F. Neese, Wiley Interdiscip. Rev.: Comput. Mol. Sci. **2**, 73 (2012).
[73]N. R. Brinkmann, G. S. Tschumper, G. Yan, and H. F. Schaefer, J. Phys. Chem. A **107**, 10208 (2003).
[74]E. Miliordos and S. S. Xantheas, J. Chem. Phys. **142**, 094311 (2015).
[75]K. A. E. Meyer and M. A. Suhm, J. Chem. Phys. **147**, 144305 (2017).
[76]Z. Xue, "Raman spectroscopy of carboxylic acid and water aggregates," Ph.D. thesis, Logos Berlin, Berlin, 2011.
[77]F. Kollipost, "Schwingungsdynamik in O–H· · · O-verbrückten Aggregaten: FTIR-Spektroskopie vom Nah- bis zum Ferninfraroten," Ph.D. thesis, Georg-August-Universität, Göttingen, 2015.
[78]C. Emmeluth and M. A. Suhm, Phys. Chem. Chem. Phys. **5**, 3094 (2003).
[79]W. H. Hocking, Z. Naturforsch., A **31**, 1113 (1976).
[80]E. Bjarnov and W. H. Hocking, Z. Naturforsch., A **33**, 610 (1978).
[81]V. Lattanzi, A. Walters, B. J. Drouin, and J. C. Pearson, Astrophys. J., Suppl. Ser. **176**, 536 (2008).
[82]G. Herzberg, *Molecular Spectra and Molecular Structure. II. Infrared and Raman Spectra of Polyatomic Molecules* (van Nostrand, New York, 1945).
[83]M. Freytes, D. Hurtmans, S. Kassi, J. Liévin, J. Vander Auwera, A. Campargue, and M. Herman, Chem. Phys. **283**, 47 (2002).
[84]A. Perrin, J. Vander Auwera, and Z. Zelinger, J. Quant. Spectrosc. Radiat. Transfer **110**, 743 (2009).
[85]S. Oswald, E. Meyer, and M. A. Suhm, J. Phys. Chem. A **122**, 2933 (2018).
[86]K. E. Otto, Z. Xue, P. Zielke, and M. A. Suhm, Phys. Chem. Chem. Phys. **16**, 9849 (2014).